Effect Of Measurement Uncertainty On Region Of Interest Based And Parametric Binding Potential Estimates For The High Resolution Research Tomograph (HRRT)

Vesna Sossi, *Member, IEEE*, Stephan Blinder, Arman Rahmim, *Member, IEEE,* Katherine Dinelle, Kevin J-C Cheng, Sarah C Lidstone

***Abstract*– High resolution Positron Emission Tomography (PET) imaging leads to very small pixel sizes. Generally the increase in resolution is not paralleled by a corresponding increase in sensitivity which may cause the count density per voxel to be low. Here we are exploring how the statistical quality of the data acquired with the high resolution research tomograph (HRRT) influences the accuracy of the determination of the binding potential (BP) for typical human studies performed with ^{11}C-raclopride. Susceptibility to noise was tested for 3 modelling approaches: the Logan graphical model, the simplified reference tissue method (RTM) and the delayed ratio method (DRM). For each approach BP was calculated on a region of interest (ROI) and voxel basis (parametric maps). Using a method based on experimentally defined replicas of time activity curves (TACs) representative of those obtained in human scans we found that for this tracer the contribution of the statistical noise to the BP determination is ~ 5-8 % when the TACs are evaluated on an ROI basis (either ROI TACs used as input, or ROI placed on the BP parametric image) and 9-12 % when calculated on a single pixel basis. The Logan approach was found to suffer from a considerable bias due to statistical noise when the BP was calculated on a single pixel basis, while RTM and DRM showed no such bias. Overall, for this tracer and these scanning conditions the RTM proved to be the least sensitive to statistical noise in the data.**

I. Introduction

High resolution Positron Emission Tomography (PET) imaging is achieved by decreasing the crystal size, thus increasing the number of possible lines of response (LORs). This leads to a decrease in the size of image voxels and a consequent increase in their number. Given that very often the amount of radioactivity injected is limited by safety regulations and that the increase in resolution tends not to be paralleled by a corresponding increase in sensitivity, the count density per voxel may be quite low. This is often the case for receptor studies acquired with the High Resolution Research Tomograph (HRRT – Siemens) (1, 2). This scanner, capable of approximately $(2.5\text{mm})^3$ resolution is currently the highest resolution human brain scanner available. Such resolution is obtained by using 119,808 detectors leading to approximately $4.5\text{x}10^9$ possible LORs when operating in full resolution mode. Data are reconstructed into 207 256x256 pixels image planes (pixel size 1.22x1.22 mm^2). Given the large number of LORs and image pixels the number of counts/voxel can be low enough to make the statistical noise in the acquired data a considerable source of uncertainty in the determination of the BP estimates.

In this study we are exploring how the statistical quality of the acquired data influences the accuracy of the determination of the binding potential (BP), which is a parameter commonly used to quantify the binding of tracers involved in reversible processes. It is known that different modelling approaches exhibit different susceptibilities to noise; we are considering the effect of noise on BP evaluated with three different, but commonly used approaches: the Logan graphical model (3), the simplified reference tissue method (RTM) (4) and delayed ratio method (DRM) (5) when calculated on a region of interest (ROI) and voxel basis (parametric maps).

The method is based on experimentally defined replicas of (TACs) representative of those obtained in human scans by extracting appropriate count rate- and number of counts-matched time frames from a dynamic study of a uniform phantom (6). This estimate does not include other sources of error such as subject motion or biological variability thus providing an intrinsic higher limit to the accuracy with which BPs can be determined.

II. Methods

A. Human studies providing TAC templates

TACs from three (S1,S2 and S3) human ^{11}C-raclopride (RAC – a D_2 receptor antagonist) scans were selected as

V.Sossi, K. Dinelle, K. J-C. Cheng, and S. Lidstone are with the University of British Columbia (UBC), Vancouver, B.C. V6T 1Z1, Canada, (e-mail vesna@phas.ubc.ca, kdinelle@phas.ubc.ca, jcheng@phas.ubc.ca., lidstone@interchange.ubc.ca)

S. Blinder is with the Pacific Parkinson's Research Centre, Vancouver, BC, V6T 1Z1 (e-mail blinder@phas.ubc.ca).

A. Rahmim is with the Department of Radiology, Johns Hopkins University School of Medicine, Baltimore, MD 21205 (e-mail arahmim1@jhmi.edu).

This work was supported by the Canadian Institute of Health Research, the TRIUMF Life Science grant, the Natural Sciences and Engineering Research Council of Canada UFA (V. Sossi), and the Michael Smith Foundation for Health Research scholarship (V. Sossi).

templates. Two subjects were injected with 10mCi (respective weights 80 kg, 68.2 kg) and one was injected with 8mCi (weight 78 kg). Data were acquired for 60 min, histogrammed into 16 frames (4x1min, 3x2min, 8x5min and 1x10 min), and reconstructed with all corrections except for decay using List Mode Ordinary Poisson (LMOP) (7). For each patient two TACs were used as templates one derived from the striatal and one from the cerebellar region. The striatal TAC was obtained from an average striatal region of interest (ROI) value (individual 207 HRRT planes were first regrouped into 68 planes by averaging 3 adjacent planes following our standard analysis protocol; four 60 mm^2 ROIs were then placed on each striatum on three adjacent regrouped planes; the template TAC was obtained from the average of these 8 ROIs x 3 planes = 24 ROIs values). The second TAC was obtained by averaging 2500 mm^2 cerebellar ROI image values over 2 adjacent regrouped planes (fig. 1)

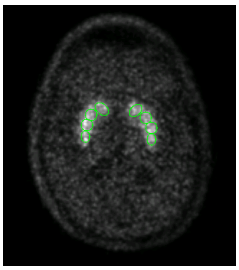

Figure 1. Example of ROIs placed on the striatal image.

B. *Phantom Studies*

Phantom. A 28 cm long 14.5x18.5 cm^2 elliptical phantom filled with an initial ^{11}C concentration of 1.13mCi/ml (total radioactivity 6.7mCi) was scanned for 4 hours (prompts count rate ranging from $1.4x10^6$ cps to 900cps). The size of the phantom was chosen so as to reproduce as best as possible the size of the human head in order to match the amount of scatter and attenuation present in a human brain scan.

TAC extraction. The data were initially histogrammed into 10 min frames and reconstructed with all corrections except decay using LMOP (7). A phantom TAC was obtained from large ROI values averaged over 61 axial central planes (fig 2 left). The radioactivity concentration values measured in the human template TACs were then used to determine those time points on the phantom TACs where the concentration matched the measured concentration in the human TAC (fig 2 middle). Phantom data acquired in a time interval around the selected time point with the interval duration matching that of the corresponding human time- frame were extracted from the phantom list mode file and reconstructed with all corrections except for decay using list mode Ordinary Poisson (LMOP) as described earlier(fig 2right).

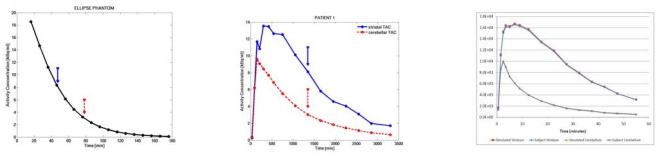

Figure 2. Phantom TAC (left). Human RAC TACs used as templates (middle) Example of a human RAC template and matching TAC obtained from the phantom study (right).

ROI placement. 120 striatal size ROIs were placed on the phantom image on the same axial planes on which the human ROIs were placed and in a very similar radial position (to match for axial sensitivity, scatter and attenuation) (fig 3). Likewise six cerebellar ROIs were drawn. TACs were calculated for each ROI.

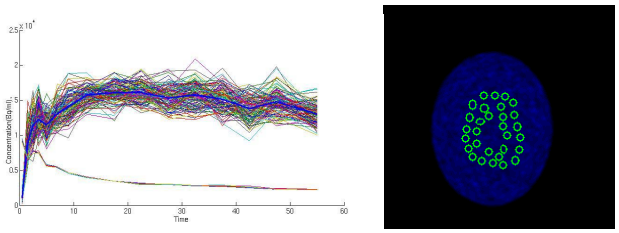

Figure 3. ROI TAC replicas differing only due to statistics for the striatum (n=120) and cerebellum (n=6). Example of ROI placement of the phantom image.

Parametric BP determination. BP was determined on a pixel basis and results were analyzed by placing the same ROIs on the parametric maps as above (by regrouping the planes ("par regroup" in Table 1), by placing them on individual planes ("par ind ROI" in Table 1) and by considering individual pixel BPs ("par pixel" in Table 1). A total of 720 individual pixels BP values were taken far enough apart to minimize correlation between pixel values.

C. *Modeling approaches*

Three commonly used modelling approaches were considered, the tissues input Logan graphical method (3), which calculates the BP as distribution volume ratio (DVR) -1, the simplified reference tissue model (RTM), which determines BP directly from the fit to the data and the delayed ratio method, where the BP is estimated as the ratio between the striatal radioactivity (averaged over the 30-60 min after injection scanning interval) and the cerebellar radioactivity (averaged over the same time) -1. The Logan approach is known to suffer a downward bias as a function of noise, so it was of interest to determine if the statistical noise alone would be sufficient to introduce bias when comparing ROI based BP values to those evaluated on individual pixels.

D. *Figures of merit*

The main figure of merit used to estimate the effect of the statistical noise on the BP determination was the coefficient of variance (COV). COV was first calculated by only varying the

phantom striatal TAC and keeping the cerebellum phantom TAC constant to estimate the effect due to the noise in the target region, then by varying the phantom cerebellar TAC and keeping the striatal TAC constant and finally overall. The secondary figure of merit was the magnitude of the BP itself used to compare the results obtained by the various methods.

III. Results and Discussion

A. BP values

Results are presented in Table 1 for the three sets of TACs derived from the three subjects (S1, S2, S3). There is good agreement between the BP evaluated on a ROI basis with the Logan and the RTM methods, while, as expected, the DRM method overestimates the BP. When the parametric BP is considered, the results produced by the various methods do not agree as well, in particular, the statistical quality of the data is low enough to introduce by itself a downward bias into the Logan BP estimate.

TABLE I
BP VALUES OBTAINED WITH THE DIFFERENT METHODS

Method	Mean BP		
	S1	S2	S3
Logan ROI	4.03	4.14	5.50
Logan par ind ROI	3.69	4.09	5.17
Logan par regroup	3.77	4.15	5.25
Logan par pixel	3.69	4.15	5.25
RTM ROI	4.13	4.16	5.41
RTM par ind ROI	4.12	4.20	5.40
RTM par regroup	4.12	4.15	5.40
RTM par pixel	4.04	4.23	5.39
DRM ROI	4.64	4.68	5.39
DRM par regroup	4.04	4.23	5.39
DRM par pixel	4.58	4.66	6.86

The bias is higher for S1 and S3 (~ 10% and 7% respectively, lower effective dose due to higher body weight) in the two lower statistics cases. Virtually no bias was observed in parametric RTM and DRM.

B. COV striatum

Results for the COV due to statistical variations in the striatal data are shown in figure 4. Logan –derived BP is most susceptible to statistical noise in the striatum, while RTM-derived BP appears the most robust with respect to striatal statistical noise, when calculated on an ROI or voxel basis. Interestingly, parametric approaches have similar COV compared to ROI based approaches when averaged over the same ROI area.

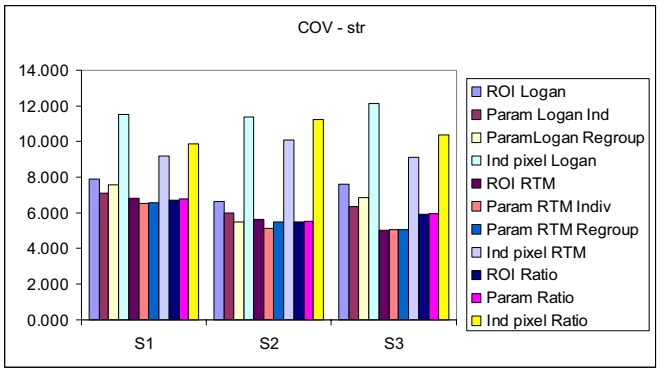

Figure 4. COV due to statistical variations in the striatal TACs. S1, S2, S3 are the three subjects, whose curves were used as templates.

C. COV cerebellum (reference region)

Results for the COVs due to statistical variations in the cerebellar data are shown in figure 5. The COVs are much smaller (~1-2%) due to the much larger ROI size. This appears in spite of the fact that the cerebellum is generally imaged closer to the axial edge of the scanner where detection sensitivity is lower. Interestingly the largest effect is observed for the DRM, which appears most susceptible to noise in the cerebellar ROI.

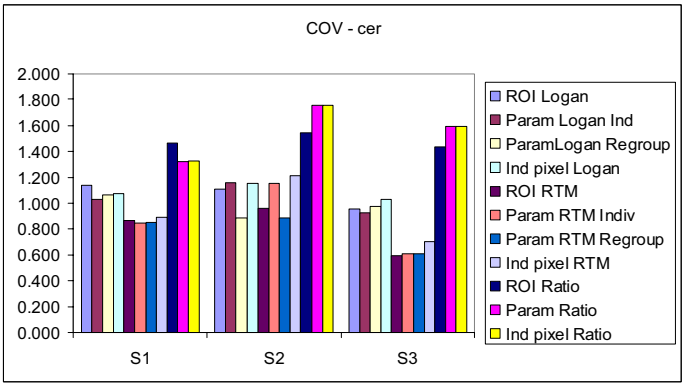

Figure 5. COV due to statistical variations in the striatal TACs. S1, S2, S3 are the three subjects, whose curves were used as templates.

D. COV overall

The results for the COV including the effect of varying the striatal and cerebellar ROIs are shown in figure 6. The RTM method is the most robust with respect to the statistical noise in the data. When data are analyzed on an ROI basis the COV varies between ~ 5%-8% and when individual pixel BPs are estimated the COV was found to vary between ~ 9-12%. In all cases the statistical noise in the striatum is the major contributor to the BP estimate uncertainty, as expected.

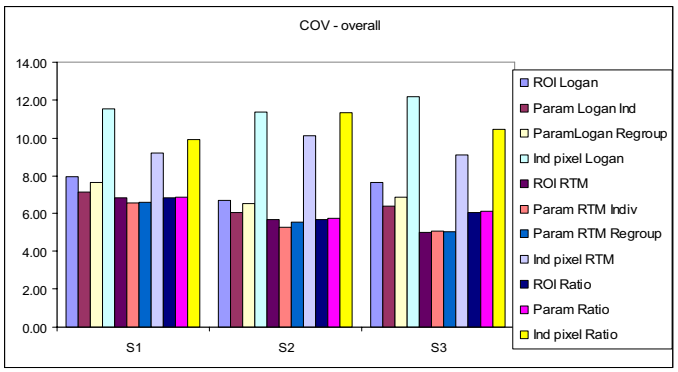

Figure 6. COV due to statistical variation in the striatal and cerebellar TACs. S1, S2, S3 are the three subjects, whose curves were used as templates.

IV. Conclusion

Using experimentally defined replicas of TACs representative of those obtained in human scans we have evaluated the contribution of the statistical noise to the BP determination in a typical RAC study when imaging with a high resolution brain tomograph. The contribution was evaluated for three different modelling approaches and for ROI and pixel based BP determination. The COV was found to be approximately 5-8 % when the data were evaluated on an ROI basis (either ROI TAC used as input, or ROI placed on the BP parametric image) and 9%-12% when calculated on a single pixel basis. The Logan approach showed a considerable bias due to statistical noise when the BP was calculated on a single pixel basis, while RTM and DRM showed no such bias. This finding indicates that when relatively small image pixel sizes are used, the number of counts per voxel can be sufficiently low to introduce enough noise to induce a downward bias in the parametric tissue input Logan approach. Other sources of noise, such as subject motion are expected to further exacerbate such bias. Overall, the RTM appeared the least sensitive to statistical noise in the data.

While these results are tracer and scanner specific, this method can be easily applied to other scanners and other tracers to determine the effect of statistical noise on a parameter estimate and/or to compare sensitivity to statistical noise between different modelling approaches.

References

[1] de Jong H, van Velden FH, Kloet RW, Performance evaluation of the ECAT HRRT: an LSO-LYSO double layer high resolution, high sensitivity scanner. Phys Med Biol. 2007 52(5) 1505-26.

[2] Sossi V, de Jong H et al., The second generation HRRT – a multi-centre scanner performance investigation et al., Nuclear Science Symposium Conference Record 2005 IEEE (4) 2195 – 2199

[3] Logan J, Fowler JS, Volkow ND et al. Distribution volume ratios without blood sampling from graphical analysis of PET data, J Cereb Blood Flow Metab. 1996 (5) 834-40.

[4] Gunn R, Lammertsma AA, Hume SP at al., Parametric imaging of ligand-receptor binding in PET using a simplified reference region model Neuroimage. 1997 6(4) 279-87

[5] Ito H, HietalaJ, Blomqvist G, et al., Comparison of the Transient Equilibrium and Continuous Infusion Method for Quantitative PET Analysis of [^{11}C]Raclopride Binding J Cereb Blood Flow Metab. 1998 (9) 941-50

[6] Sossi V, Camborde M-L, Tropini G et al., The influence of measurement uncertainties on the evaluation of the distribution volume ratio and binding potential in rat studies on a microPET R4: a phantom studyPhys Med Biol. 2005 (50) 2859-69

[7] Rahmim A, Cheng K J-C, Blinder S et al., dynamic image reconstruction in state-of-the-art high resolution PET Phys. Med. Biol. 2005 (50) 4887-4912